

# Theoretical He I Emissivities in the Case B Approximation

R. L. Porter, R. P. Bauman, G. J. Ferland, & K. B. MacAdam

*Dept. of Physics and Astronomy, University of Kentucky, Lexington, KY, 40506*

rporter@pa.uky.edu

## ABSTRACT

We calculate the He I case B recombination cascade spectrum using improved radiative and collisional data. We present new emissivities over a range of electron temperatures and densities. The differences between our results and the current standard are large enough to have a significant effect not only on the interpretation of observed spectra of a wide variety of objects but also on determinations of the primordial helium abundance.

*Subject headings:* atomic data—atomic processes—ISM: atoms—ISM: clouds—plasmas

## 1. Introduction

Helium is the second most abundant element in the universe, and its emission and opacity help determine the structure of any interstellar cloud. Its abundance relative to hydrogen can be measured within a few percent since the emissivities of H I and He I lines have similar dependences on temperature and density. This makes it an indicator of both stellar and primordial nucleosynthesis (Pagel 1997).

A good discussion of the history of calculations of the helium recombination spectra is given by Benjamin, Skillman, & Smits (1999, hereafter BSS99), who present new calculations - the current standard in the field. Yet much progress has been made since the work by Smits (1991, 1996) upon which the BSS99 results depend. We implement these improvements, present a new set of predictions, and compare our results with those of BSS99. The differences are large enough to impact continuing attempts to estimate the primordial helium abundance (Peimbert *et al* 2002).

## 2. The New Model Helium Atom

The basic physical processes have been described by Brocklehurst (1972) and BSS99. Here we will describe the differences between BSS99 and our new numerical representation of the helium atom, which is a part of the spectral simulation code Cloudy (Ferland *et al* 1998). This model resolves all terms,  $nLS$ , up to an adjustable maximum principal quantum number  $n_{max}$ , followed by a pseudolevel,  $n_{max} + 1$ , in which all  $LS$  terms are assumed to be populated according to statistical weight and “collapsed” into one. We set recombinations into the collapsed level equal to the convergent sum of recombinations from  $n = n_{max} + 1$  to  $\infty$ . In the low-density limit, the collapsed level increases the emissivities of our benchmark lines (the same 32 lines given in BSS99) by 0.4%, on average, with  $n_{max}=100$ . The decays from states with  $l = n - 1$  are most sensitive to this correction for system truncation. The strong optical line  $\lambda 5876$  is corrected upward by 1.3%. At finite densities collisional processes force the populations of very highly excited states into local thermodynamic equilibrium (LTE). In this case the adequacy of the method used to compensate for truncation is unimportant. We find the corrections negligible for  $n_e = 100 \text{ cm}^{-3}$  and  $n_{max}=100$ . Consequently, the uncertainties in the results presented in Section 3 are due to the uncertainties in atomic data, especially the often substantial uncertainties in collisional rates affecting terms not in LTE at given conditions.

There are several differences in atomic data for radiative processes between BSS99 and the present work. The transition probabilities and radiative recombination coefficients are obtained from oscillator strengths and photoionization cross-sections. BSS99 uses the oscillator strengths calculated by Kono & Hattori (1984). While these agree very well with the essentially exact oscillator strengths of Drake (1996), Drake presents a much larger set, up to and including  $n=10$  and  $l=7$ , which we adopt. Hummer & Storey (1998, hereafter HS98) have presented *ab initio* calculations of threshold photoionization cross-sections up to  $n=4$ . BSS99 uses cross-sections from TOPbase<sup>1</sup> (Cunto, 1993), while we use the more accurate HS98 values. The dominant remaining uncertainties in radiative data are in oscillator strengths involving low  $l$  states (with  $n > 10$ ) and photoionization cross-sections for low  $l$  states (with  $n > 4$ ). HS98 also illustrates the method, originally discussed by Seaton (1958), of calculating threshold photoionization cross-sections by extrapolating absorption oscillator strengths to the threshold energy of a given level. This method has been used in the present work, based on the oscillator strengths from Drake, to extend the *ab initio* cross-sections of HS98 to greater  $n$ .

Differences in collisional data between BSS99 and the current work are also significant.

---

<sup>1</sup><http://vizier.u-strasbg.fr/topbase/topbase.html>

For low- $n$  transitions for which there are *ab initio* calculations, BSS99 uses the collision strengths of Sawey & Berrington (1993). We replace these, where available, with the results of the close-coupling calculation by Bray *et al* (2000), which include continuum states not considered in the  $R$ -matrix calculations by Sawey & Berrington. For  $l$ -changing collisions BSS99 uses two different treatments: Seaton (1962, hereafter S62) for low- $l$  transitions, and Pengelly & Seaton (1964, hereafter PS64) otherwise. Neither of these treatments allows for angular momentum transfers greater than one unit, and both apply when the projectile velocity is greater than the velocity of the bound electron. The r.m.s. electron and projectile velocities in conditions considered by BSS99, assuming proton colliders, are

$$v_e = \frac{Z\alpha c}{n} \text{ and } v_{proj} = \sqrt{\frac{3kT}{m_p}}, \quad (1)$$

where  $\alpha$  is the fine structure constant,  $c$  is the speed of light, and  $Z$  is the screened nuclear charge. Dividing the latter by the former, we arrive at the expected value of the reduced velocity as a function of temperature and principal quantum number

$$\langle \tilde{v} \rangle = \frac{v_{proj}}{v_e} = 7.19 \times 10^{-5} n \sqrt{T(\text{K})}. \quad (2)$$

For typical nebular temperatures this reduced velocity will be of order or less than unity for proton colliders for all  $n \leq 150$ ; the treatment of PS64 is applicable only for greater  $n$ , and it greatly overestimates  $l$ -mixing cross-sections when used outside its range of validity (MacAdam, Rolfes, & Crosby 1981).

Vrinceanu & Flannery (2001, hereafter VF01) give a (classical) theory of  $l$ -changing collisions and claim exact solutions in the limit that the intrashell transition is induced by slow distant collisions. Their treatment allows naturally for angular momentum changes greater than unity. (At a sufficiently high reduced velocity large angular momentum transfers are strongly suppressed and the theory goes to the optically allowed limit with which PS64 is concerned.) We use equation 41 of Kazansky & Ostrovsky (1996) for the angle,  $\Delta\Phi$ , swept out by the projectile. A physical basis for the necessary large impact parameter cutoff in the theory follows from equating the Stark and quantum-defect precession frequencies. The Stark frequency is given by

$$\omega_s = \frac{3Z_1 n}{2b^2} a.u., \quad (3)$$

and the quantum-defect precession frequency (Hezel *et al* 1992) is given by

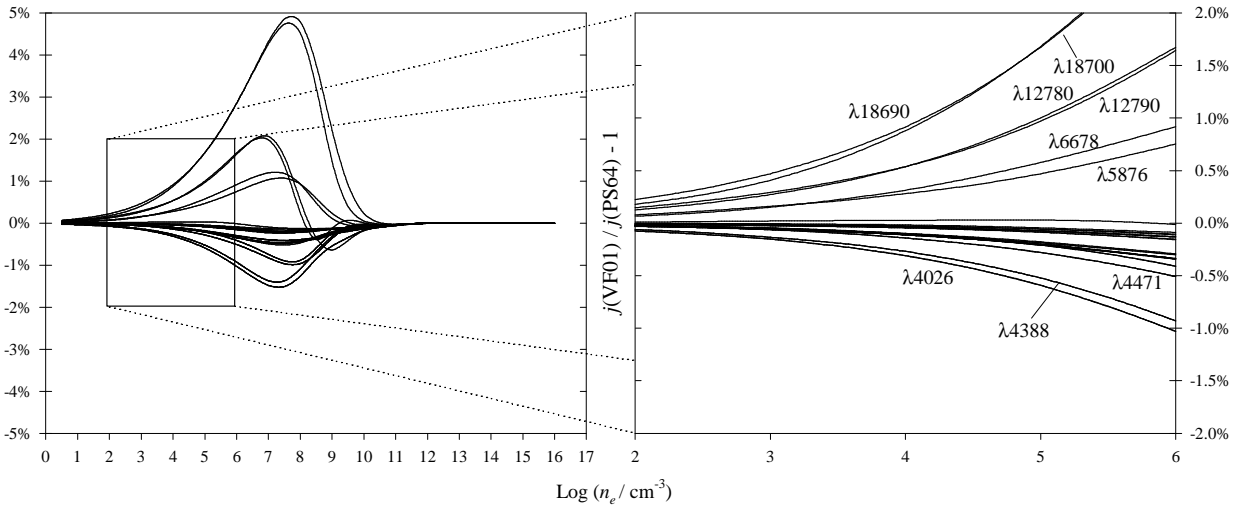


Fig. 1.— Percent difference between the emissivities calculated using two different Stark collision treatments, for several strong lines, as a function of  $n_e$ . Left panel: a wide range of densities - as expected, there is no effect in either the low density extreme, because the collision rates are negligible, or the high density extreme, where the Stark collisions force the terms to LTE. The majority of lines are most sensitive at densities found in stellar envelopes and quasar emission line regions. Right panel: the range of densities found in nebulae - several lines have a sensitivity to the Stark collision treatment of about 1%.

$$\omega_{qd} = \frac{5\delta_l}{n^3l} \left(1 - \frac{3l^2}{5n^2}\right) a.u. \quad (4)$$

where  $\delta_l$  is the quantum defect,  $Z_1$  is the charge of the projectile and  $b$  is the impact parameter. By setting  $\omega_{qd}$  equal to  $\omega_s$ , we obtain a maximum impact parameter,  $b_{max}$ . The electron orbit precession will be faster than the Stark beating at larger impact parameters, so that transitions are increasingly less likely. To insure symmetry, we use the average  $\omega_{qd}$  of the initial and final levels. We use VF01 for  $l$ -changing collisions involving initial and final levels with  $l \geq 3$ , and like BSS99 we use the impact parameter treatment of S62 for  $l$ -change from  $s$ ,  $p$ , and  $d$  levels. We use electron, proton and  $\text{He}^+$  colliders for all transitions, taking  $n_{\text{He}^+} = 0.1 n_p$  and  $n_e = n_p + n_{\text{He}^+}$ . Since S62, which describes electron collisions, is based upon the method of virtual quanta (see Jackson 1999), we can readily adapt it for the positive-ion collisions: The power spectrum of the time-dependent fields generated at the target atom by a passing charged projectile depends only on the projectile's charge magnitude, speed (not kinetic energy or mass separately) and impact parameter. The same considerations apply to PS64 and VF01 and have been implemented to allow for all three collider species. In calculating the necessary thermal averages we have assumed that the same temperature characterizes electrons, protons and  $\text{He}^+$  ions.

Figure 1 compares emissivities we predicted using the VF01 and PS64 theories. The predicted emissivities typically change by about 1% for nebular densities by using the theory of VF01 rather than that of PS64. The difference is much greater at high densities found, for example, in parts of quasars.

### 3. Results

In Figure 2 we compare our results with those of BSS99 for the case  $T_e = 10^4$  K and  $n_e = 10^4 \text{ cm}^{-3}$ . The average difference for the 32 emission lines is 4.6%. The greatest difference is for  $\lambda 4121$ , for which our emissivity is 25% greater. In general, agreement worsens with increasing density; at  $n_e = 10^2 \text{ cm}^{-3}$ , the average and greatest differences are 1.6% and 6.4%, respectively, while at  $n_e = 10^6 \text{ cm}^{-3}$ , we find differences of 7.0% and 35%. Agreement also worsens with increasing temperature. Table 1 presents emissivities for all of the temperatures and densities considered by BSS99. We believe that these results are a significant improvement. The application of these results to specific astrophysical problems will be the subject of future papers.

We thank G. W. F. Drake for making available extensive tables of his calculations, D. Vrinceanu and M. J. Cavagnero for helpful discussions, and P. J. Storey, whose constructive

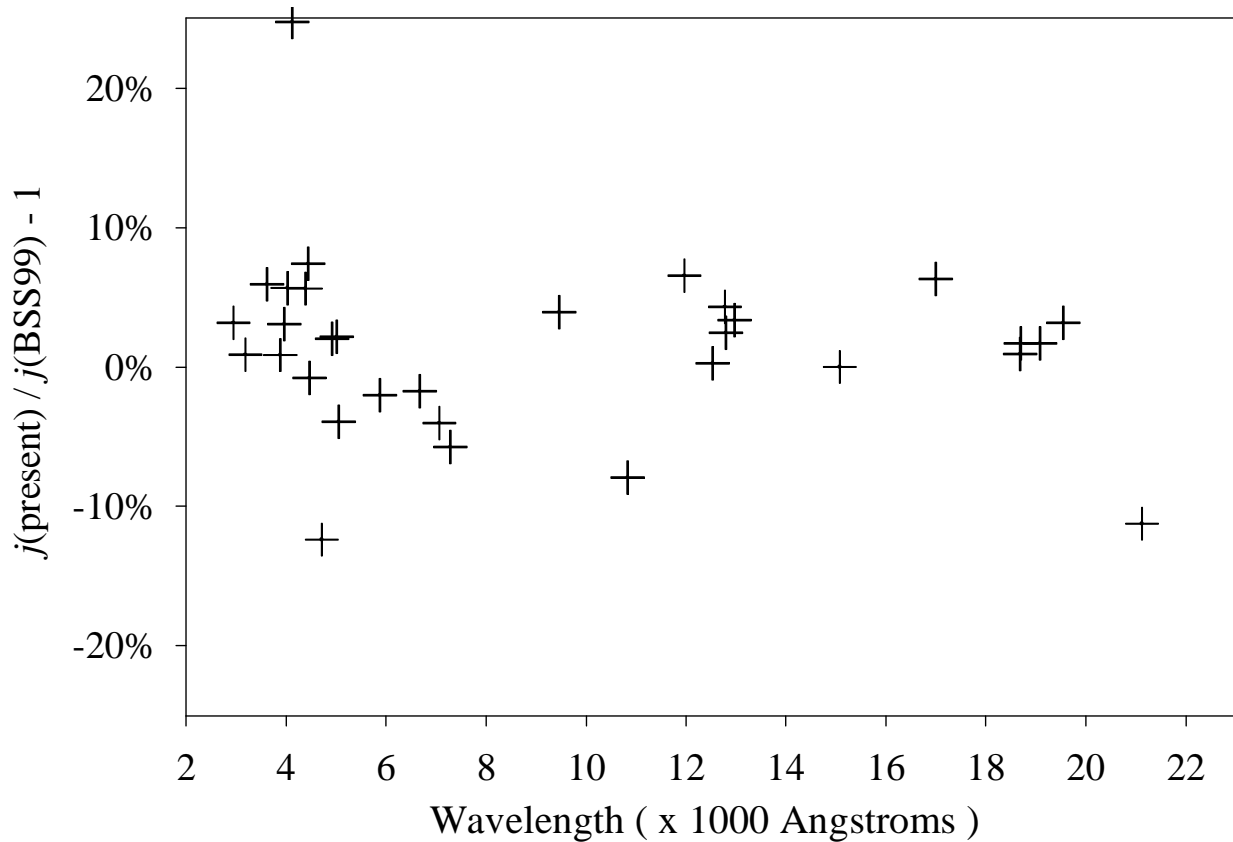


Fig. 2.— A comparison of the present results with those of BSS99 at  $T_e = 10^4$  K and  $n_e = 10^4$  cm $^{-3}$ .

criticisms helped us to significantly improve our work. We also acknowledge support from NASA grant NAG5-12020 and NSF grant AST 0307720.

## REFERENCES

- Benjamin, R. A., Skillman, E. D., & Smits, D. P. 1999, ApJ 514, 307
- Bray, I., Burgess, A., Fursa, D. V., & Tully, J. A., 2000, A&AS 146, 481-498
- Brocklehurst, M. 1972, MNRAS 157, 211
- Cunto, W., Mendoza, C., Ochsebein, F., & Zeippen, C. J. 1993, A&A 275, L5
- Drake, G. W. F. 1996, in Atomic, Molecular, & Optical Physics Handbook, ed. G. W. F. Drake (New York: AIP Press), 154. (Actual oscillator strengths taken from tables received via private communication from Drake.)

- Ferland, G. J., Korista, K. T., Verner, D. A., Ferguson, J. W., Kingdon, J. B., & Verner, E. M. 1998, PASP 110, 761-778
- Hezel, T. P., Burkhardt, C. E., Ciocca, M., He, L-W., & Leventhal, J. J. 1992, Am. J. Phys. 60, 329
- Hummer, D. G. & Storey, P. J. 1998, MNRAS 297, 1073
- Jackson, J. D. 1999, Classical Electrodynamics, 3rd edition (New York: John Wiley & Sons)
- Kazansky, A. K. & Ostrovsky, V. N. 1996, JPhysB: At. Mol. Opt. Phys. 29, 3651
- Kono, A. & Hattori, S. 1984, PhysRevA 29, 2981
- MacAdam, K. B., Rolfes, R., & Crosby, D. A. 1981, PhysRevA 24, 1286
- Pagel, B. E. J. 1997, Nucleosynthesis and Chemical Evolution of Galaxies, (Cambridge; Cambridge University Press)
- Peimbert, A., Peimbert, M., & Luridiana, V. 2002, ApJ 565, 668
- Pengelly, R. M., & Seaton, M. J. 1964, MNRAS 127, 165
- Sawey, P. M. J., & Berrington, K. A. 1993, ADNDT 55, 81
- Seaton, M. J. 1958, MNRAS 118, 504
- Seaton, M. J. 1962, Proc. Phys. Soc. 79, 1105
- Smits, D. P. 1991, MNRAS 248, 193
- Smits, D. P. 1996, MNRAS 278, 683
- Vrinceanu, D. & Flannery, M. R. 2001, PhysRevA 63, 032701

Table 1. He I Case B Emissivities.

$\lambda(\text{\AA})$	$T_e$ (K):	5000			10000			20000		
	$n_e$ ( $\text{cm}^{-3}$ ):	$10^2$	$10^4$	$10^6$	$10^2$	$10^4$	$10^6$	$10^2$	$10^4$	$10^6$
2945		0.4142	0.4261	0.4567	0.2687	0.2816	0.2958	0.1648	0.1987	0.2112
3187		0.8693	0.8950	0.9594	0.5617	0.6119	0.6507	0.3432	0.4584	0.4963
3614		0.1115	0.1151	0.1241	0.0691	0.0717	0.0752	0.0397	0.0471	0.0496
3889		2.2452	2.3261	2.5038	1.4116	1.6794	1.8348	0.8315	1.3332	1.4859
3965		0.2280	0.2353	0.2532	0.1409	0.1471	0.1543	0.0807	0.0966	0.1020
4026		0.5279	0.5427	0.5866	0.2917	0.3029	0.3175	0.1457	0.1782	0.1896
4121		0.0341	0.0348	0.0363	0.0249	0.0300	0.0323	0.0184	0.0338	0.0379
4388		0.1411	0.1453	0.1568	0.0772	0.0798	0.0834	0.0380	0.0445	0.0468
4438		0.0145	0.0149	0.0157	0.0101	0.0111	0.0117	0.0070	0.0100	0.0107
4471		1.1469	1.1781	1.2699	0.6124	0.6465	0.6806	0.3010	0.4077	0.4418
4713		0.0904	0.0929	0.0977	0.0652	0.0833	0.0917	0.0478	0.0957	0.1087
4922		0.3132	0.3222	0.3463	0.1655	0.1722	0.1801	0.0799	0.0973	0.1027
5016		0.5849	0.6039	0.6498	0.3539	0.3808	0.4035	0.1996	0.2554	0.2735
5048		0.0355	0.0366	0.0387	0.0244	0.0281	0.0301	0.0167	0.0253	0.0276
5876		3.3613	3.4419	3.6889	1.6344	1.8724	2.0179	0.7887	1.4753	1.6649
6678		0.9640	0.9872	1.0512	0.4629	0.4962	0.5223	0.2170	0.3082	0.3250
7065		0.4273	0.4750	0.5303	0.2997	0.5897	0.7166	0.2154	0.6809	0.8096
7281		0.1318	0.1387	0.1497	0.0886	0.1203	0.1357	0.0593	0.1086	0.1227
9464		0.0229	0.0235	0.0252	0.0148	0.0155	0.0163	0.0091	0.0109	0.0116
10830		4.9896	13.9601	21.4091	3.3152	18.8390	25.4507	2.3419	18.8421	23.6646
11970		0.0532	0.0547	0.0591	0.0294	0.0305	0.0320	0.0146	0.0179	0.0191
12530		0.0278	0.0286	0.0307	0.0179	0.0195	0.0208	0.0109	0.0146	0.0158
12780		0.2010	0.2056	0.2196	0.0936	0.0972	0.1011	0.0410	0.0513	0.0546
12800		0.0670	0.0686	0.0728	0.0311	0.0320	0.0330	0.0137	0.0169	0.0175
12970		0.0178	0.0183	0.0198	0.0097	0.0101	0.0105	0.0048	0.0056	0.0059
15080		0.0121	0.0125	0.0134	0.0074	0.0078	0.0082	0.0042	0.0051	0.0054
17000		0.0811	0.0833	0.0898	0.0433	0.0457	0.0481	0.0212	0.0288	0.0312
18680		0.5062	0.5126	0.5412	0.2184	0.2282	0.2367	0.0955	0.1261	0.1324
18700		0.1687	0.1711	0.1793	0.0727	0.0748	0.0768	0.0321	0.0449	0.0445
19090		0.0289	0.0297	0.0319	0.0152	0.0159	0.0166	0.0073	0.0089	0.0094
19550		0.0162	0.0167	0.0179	0.0104	0.0114	0.0121	0.0064	0.0085	0.0092
21120		0.0138	0.0141	0.0149	0.0099	0.0127	0.0139	0.0073	0.0146	0.0166

Note. — Emissivities  $4\pi j_\lambda/n_e n_{He^+}$  are given in units  $10^{-25}$  erg  $\text{cm}^3$   $\text{sec}^{-1}$ . The hydrogen density is  $0.9 n_e$ , and the helium abundance is one-tenth of the hydrogen abundance.